

PERIODICALLY GAPPED DATA SPECTRAL VELOCITY ESTIMATION IN MEDICAL ULTRASOUND USING SPATIAL AND TEMPORAL DIMENSIONS

Paul Liu* and Dong Liu†

*Saset (Chengdu) Inc., Chengdu, China

†College of Computer Science, Sichuan University, Chengdu, China

ABSTRACT

Modern medical ultrasound scanners estimate blood velocity distribution by computing the spectrogram of a temporal data sequence, typically using periodogram methods which require long observation windows. Furthermore, an additional B-mode image is often displayed, resulting in gaps in the data at B-mode emissions. We propose a data-adaptive velocity estimator for periodically gapped (PG) data that extends PG-Capon and PG-APES by using two dimensional spatial and temporal data to estimate a one dimensional spectrum. We show through realistic flow simulations that our method improves spectral resolution and reduces leakage in comparison to PG-Capon, PG-APES, and correlogram based gapped data velocity estimators, potentially increasing the maximum detectable velocity and temporal resolution of blood flow using ultrasound.

Index Terms— gapped data spectral estimation, blood velocity estimation, medical ultrasound

1. INTRODUCTION

Spectrum Doppler is a medical ultrasound mode that estimates blood and tissue velocity. A sinusoidal pulse of several cycles is emitted and the received echo is called the fast-time, or axial, signal. At a selected depth, samples within a range gate are recorded and averaged, yielding one temporal sample per emission. Although averaging is sub-optimal, it is simple. The process is repeated many times with subsequent emissions fired at the rate of the pulse repetition frequency (PRF). The slow-time, or temporal, signal sampled at the PRF has a spectrum proportional to the velocity distribution of the flow. The spectrum is evaluated at different times to create a spectrogram that reflects the time-varying velocity distribution of in-vivo flow.

In commercial systems, the spectrum is typically estimated with an averaged periodogram, or Welch's method. [1] Such Fourier Transform based methods suffer from poor resolution or leakage, requiring a large observation window and hence lowering the frame rate. Data dependent spectral estimators such as Capon and amplitude and phase estimation (APES) [2] offer much higher resolution and reduces the

observation window. Gran et al. proposed modified Capon and APES estimators called Blood Power Capon (BPC) and Blood spectral APES (BAPES) [3] in which the correlation matrix uses spatial, or fast time, information in addition to the temporal signal to improve the accuracy of the estimation.

In addition to estimating and displaying the spectrogram, ultrasound systems often run in duplex mode where a B-mode image is displayed with the spectrogram. B-mode emissions are interleaved with Doppler emissions, and depending on the ratio between B-mode and Doppler emissions, there may be gaps in the Doppler emissions. For spectral estimation with missing data, a correlogram based method that weights each lag based on available observations is proposed in [4]. However, it suffers from the same resolution problems as other Fourier based methods. GAPES, an extension of APES to gapped data [5] is based on interpolation of the missing samples and has the resolution of APES and can handle quite general sampling patterns. However it is computationally heavy and cannot be extended to the Capon method. PG-Capon and PG-APES is an interpolation free and extension to periodically gapped (PG) data that may be orders faster than GAPES [6].

We propose an extension of PG-Capon and PG-APES called BPG-Capon and BPG-APES respectively. Temporal samples from different depths, after a correction to depth dependent phase shift, are used as additional minimization criteria. In the special case of no gaps, BPG-APES reduces to BAPES of [3]. Using simulated Field II flow data of a time-varying flow [7], we show an improvement in main lobe width and leakage over conventional PG estimators and the correlogram method.

2. THEORY AND METHODS

Defining depth as z-axis, axial (depth) velocity v_z at the interrogated location is determined from slow-time samples $x_d(n)$, corresponding to emission n at fast-time (depth sample) d . $x_d(n)$ can be expressed by its analytic (but not baseband) representation as [8]

$$x_d(n) = \alpha_{v_z} \exp \left[j2\pi \left(d \frac{f_c}{f_s} - n \frac{2f_c v_z}{c f_{prf}} \right) \right] + e_{v_z, d}(n) \quad (1)$$

for $d = 0, \dots, D-1$ and $n = 0, \dots, N$, where α_{v_z} is the complex amplitude of the complex sinusoid at velocity v_z , $e_{v_z,d}(n)$ is the residual term consisting of all signals at velocities different from v_z and system noise, f_c is the transducer center frequency, f_s is the system sampling frequency, f_{prf} is the pulse repetition frequency, and c is the speed of sound in the body. Velocity is assumed to be constant in both the slow-time observation window of length N and fast-time window of length D , also called range gate. The observation window is then shifted in slow-time to create the next vertical spectrum slice in the spectrogram. Estimating the blood velocity distribution is then a problem of estimating $|\alpha_{v_z}|^2$ for each velocity of interest. After the substitution $\omega = -4\pi f_c v_z / c f_{prf}$ and $\phi = 2\pi f_c / f_s$, we have

$$x_d(n) = \alpha_\omega e^{j\phi d + j\omega n} + e_{\omega,d}(n) \quad (2)$$

By interleaving B-mode and Doppler emissions in a periodic pattern, such as $v v v b v v v b \dots$ where v denotes Doppler emission, b is a B-mode emission, $v v v b$ is a cluster of periodicity 4 with 3 available samples and 1 missing sample. The Doppler samples $x_d(n)$ exist for all d and n but are available only for

$$\begin{aligned} n &= 0, \dots, N_s - 1, \\ N_p, \dots, N_p + N_s - 1, \\ &\vdots \\ (N_c - 1)N_p, \dots, (N_c - 1)N_p + N_s - 1 \end{aligned} \quad (3)$$

and all d . N_p is the periodicity of the clusters, N_s is the number of available samples per cluster, and N_c is the total number of clusters. Therefore, $N_a = N_c N_s$ samples are available for each depth.

Following [6] and defining \tilde{N}_c and \tilde{N}_s as two user chosen parameters, we divide the data into DL so-called snapshots $\mathbf{x}_d(l)$ of length $M = \tilde{N}_c \tilde{N}_s$ where $L = (N_s - \tilde{N}_s + 1)(N_c - \tilde{N}_c + 1)$ and

$$\mathbf{x}_d(l) = [x_d(k_l + m_0) \ x_d(k_l + m_1) \ \dots \ x_d(k_l + m_{M-1})]^T \quad (4)$$

for $l = 0, \dots, L-1$, where k_l and m_l are vectors of indices

$$\begin{aligned} k_l &= \{0, 1, \dots, N_s - \tilde{N}_s, \\ &N_p, N_p + 1, \dots, N_p + N_s - \tilde{N}_s, \dots \\ &(N_c - \tilde{N}_c)N_p, (N_c - \tilde{N}_c)N_p + 1, \dots, \\ &(N_c - \tilde{N}_c)N_p + N_s - \tilde{N}_s\} \\ m_l &= \{0, 1, \dots, \tilde{N}_s - 1, \\ &N_p, N_p + 1, \dots, N_p + \tilde{N}_s - 1 \\ &(\tilde{N}_c - 1)N_p, (\tilde{N}_c - 1)N_p + 1, \dots, \\ &(\tilde{N}_c - 1)N_p + \tilde{N}_s - 1\} \end{aligned} \quad (5)$$

Now form the following matrices

$$\mathbf{X}_d \triangleq [\mathbf{x}_d(0) \ \dots \ \mathbf{x}_d(L-1)] \quad (6)$$

$$\mathbf{X} \triangleq [\mathbf{X}_0 \ \dots \ \mathbf{X}_{D-1}] \quad (7)$$

where \mathbf{X}_d is a $M \times L$ matrix whose l 'th column is $\mathbf{x}_d(l)$ and \mathbf{X} is a $M \times DL$ matrix of \mathbf{X}_d 's stacked row-wise. Similarly, define $\mathbf{E}_{\omega,d} \triangleq [\mathbf{e}_{\omega,d}(0) \ \dots \ \mathbf{e}_{\omega,d}(L-1)]$ and $\mathbf{E}_\omega \triangleq [\mathbf{E}_{\omega,0} \ \dots \ \mathbf{E}_{\omega,D-1}]$. Let

$$\mathbf{A}_d(\omega) \triangleq \mathbf{a}_M(\omega) \mathbf{a}_{L,d}^T(\omega) \quad (8)$$

$$\mathbf{A}(\omega) \triangleq \mathbf{a}_M(\omega) \mathbf{a}_L^T(\omega) \quad (9)$$

where

$$\mathbf{a}_M(\omega) \triangleq [e^{j\omega m_0} \ \dots \ e^{j\omega m_{M-1}}]^T \quad (10)$$

$$\mathbf{a}_{L,d}(\omega) \triangleq [e^{j\omega k_0 + j\phi d} \ \dots \ e^{j\omega k_{L-1} + j\phi d}]^T \quad (11)$$

$$\mathbf{a}_L(\omega) \triangleq [\mathbf{a}_{L,0}(\omega)^T \ \dots \ \mathbf{a}_{L,D-1}(\omega)^T]^T \quad (12)$$

and phase shift caused by depth is incorporated into $\mathbf{a}_L(\omega)$ rather than $\mathbf{a}_M(\omega)$. $\mathbf{a}_L(\omega)$ consists of D complex sinusoids with incremental phase shift ϕ stacked on each other column-wise. We can write (2) as

$$\mathbf{X} = \alpha(\omega) \mathbf{A}(\omega) + \mathbf{E}(\omega) \quad (13)$$

and interpret the estimation of $\alpha(\omega)$, which is assumed to be constant over the temporal and spatial observation window, as a linear regression between $\alpha(\omega)$ and the spatial and temporal available data matrix \mathbf{X} . Because the DL residual vectors $\mathbf{e}_{\omega,d}(l)$ are correlated, we compute the weighted least-squares (WLS) estimate of $\alpha(\omega)$ as

$$\hat{\alpha}(\omega) = \operatorname{argmin}_{\alpha(\omega)} \|\mathbf{W}^{-1/2}(\mathbf{X} - \alpha(\omega) \mathbf{A}(\omega))\|^2 \quad (14)$$

where $\|\cdot\|$ is the Froebenius norm and $(\cdot)^{-1/2}$ is the Hermitian square root of a positive definite matrix. The weighting matrix \mathbf{W} essentially whitens the residuals $e_{\omega,d}(n)$ within an individual residual vector $\mathbf{e}_{\omega,d}(l)$ but not necessarily between vectors. If the transformed residuals are uncorrelated with each other and have equal mean and variance, then by the Gauss-Markov theorem, $\hat{\alpha}(\omega)$ is the best linear unbiased estimator (BLUE). In practice, we can approximate but not guarantee the aforementioned conditions, but nevertheless arrive at a ‘‘good’’ solution. The solution to (14) is [6]

$$\hat{\alpha}(\omega) = \frac{\mathbf{a}_M^H(\omega) \mathbf{W}^{-1} \mathbf{g}(\omega)}{\mathbf{a}_M^H(\omega) \mathbf{W}^{-1} \mathbf{a}_M(\omega)} \quad (15)$$

where

$$\mathbf{g}(\omega) \triangleq \frac{1}{DL} \mathbf{X} \mathbf{a}_L^c(\omega) \quad (16)$$

where $(\cdot)^c$ denotes complex conjugate and $(\cdot)^H$ denotes Hermitian tranpose.

We obtain a collection of methods by choosing different \mathbf{W} , \mathbf{X} and \mathbf{a}_L :

BPG-Capon: Our proposed estimator uses available 2-D data to solve a 1-D spectrum estimation problem in which a phase difference between depth samples needs is accounted for.

$$\mathbf{W}_{BPGC} = \frac{1}{DL} \mathbf{X} \mathbf{X}^H \triangleq \hat{\mathbf{R}} \quad (17)$$

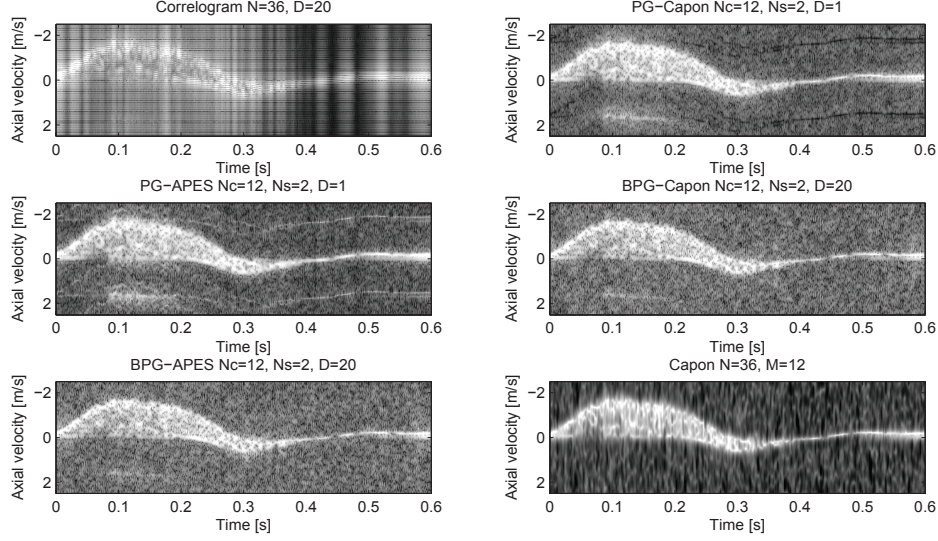


Fig. 1. Comparison of spectrograms for an unsteady flow using observation windows of the same length of 36 obtained using different gapped data estimators. With the exception of the reference Capon spectrogram of non-missing data, all spectrograms are computed from data where every third sample is missing. D denotes the number of depth samples used in the estimators.

BPG-APES: We can choose a data-dependent weight

$$\mathbf{W}_{BPGA}(\omega) = \hat{\mathbf{R}} - \frac{1}{D} \mathbf{g}(\omega) \mathbf{g}^H(\omega) \triangleq \hat{\mathbf{Q}}(\omega) \quad (18)$$

PG-Capon and *PG-APES:* For a fixed depth $d_0 = \lfloor D/2 \rfloor$, we get the purely 1-D original PG estimators.

$$\mathbf{W}_{PGC} = \frac{1}{L} \mathbf{X}_{d_0} \mathbf{X}_{d_0}^H \triangleq \hat{\mathbf{R}}_{d_0} \quad (19)$$

$$\mathbf{W}_{PGA}(\omega) = \hat{\mathbf{R}}_{d_0} - \mathbf{g}_{d_0}(\omega) \mathbf{g}_{d_0}^H(\omega) \quad (20)$$

where $\mathbf{g}_d(\omega) \triangleq \frac{1}{L} \mathbf{X}_d \mathbf{a}_{L,d}^c(\omega)$.

BAPES: The Blood spectral APES proposed in [3] is for conventional, non-missing data velocity estimation. Here, $N_c = 1$, $\tilde{N}_c = 1$, $\tilde{N}_s = M$, and $N_s = N$ because there are no gaps. We still form \mathbf{X}_d 's and \mathbf{X} with (6) and (7).

$$\mathbf{W}_{BAPES} = \hat{\mathbf{Q}}(\omega) \quad (21)$$

BPC: Blood spectral Power Capon [3] uses the estimator

$$\hat{\alpha}(\omega) = \frac{1}{\mathbf{a}_M^H(\omega) \hat{\mathbf{R}}^{-1} \mathbf{a}_M(\omega)} \quad (22)$$

We will compare the methods to a non-data adaptive velocity estimator [4] based on the correlogram

$$\hat{\alpha}(\omega) = \sum_{u=-(N-1)}^{N-1} \hat{R}(u) e^{-j\omega u} \quad (23)$$

$$\hat{R}(u) = \frac{1}{DA(u)} \sum_{d=0}^{D-1} \sum_{n=0}^{N-1-d} x_d^*(n) x_d(n+u) \quad (24)$$

where $A(u)$ denotes the number of available lag estimate pairs $x_d^*(n) x_d(n+u)$ where both samples are not missing, for a fixed d .

3. RESULTS AND DISCUSSION

We evaluate the performance of the estimators with realistic simulated flow with time-varying velocity distribution using the Field II package [7]. We use an existing implementation¹ of a cylindrical vessel flow profile based on the Womersley model [9] for pulsating flow from the femoral artery. The flow model is highly pulsating and will test the estimators' ability to handle rapid velocity variations. A 5MHz 64 element linear array transducer was simulated with an excitation waveform of a four cycle sinusoid at the transducer center frequency. The PRF was 15 KHz and the system sampling frequency was 100 MHz. The received RF lines were Hilbert transformed to create the in-phase and quadrature components. Additive white zero mean circularly symmetric Gaussian noise was added at a SNR of 50 dB. Clutter filtering may be done in the frequency domain by zeroing low frequencies.

For generating the spectrograms of Figure 1, missing samples were zeroed out with the periodic pattern of 1 1 0 1 1 0 ... where 1 denotes an available sample and 0 denotes a missing sample. We use a series of methods all using an obser-

¹<http://server.elektro.dtu.dk/personal/jaj/field/>

vation window of $N = 36$. With every third sample missing, gapped data estimators only have 24 available samples. For methods that require depth samples, we use $D = 20$ samples. The depth-averaged correlogram estimator performs well for a long observation window (> 100) but suffers from poor resolution and high noise estimates when using short observation windows. For the periodic gapped data techniques, we have in each observation window $N_c = 12$ clusters of length $\hat{N}_c = 2$ with $N_s = 2$ and $\hat{N}_s = 2$. Estimators that use depth information are less vulnerable to aliasing effects and have improved spectral resolution. Finally as a reference, we perform a conventional Capon estimate with no missing estimates of order 12.

For display, the spectrums are log transformed and the lowest 0.005 and highest 0.995 values are clipped because blood spectrum is assumed to be non-spiky. Therefore outliers do not offer any relevant information and only reduce contrast. The spectrograms are then displayed with a large dynamic range of 80 dB for comparison. In practice, using a smaller dynamic range will threshold lower pixel intensities and create a cleaner image, but such processing will mask the true performance of the methods.

In Figure 2, we plot the spectrum corresponding to peak systole at $t=0.12s$ from Figure 1 and compare main lobe width and leakage levels. For the spectral peak at -1.3 m/s, the main lobe width is smallest for the Capon estimator, largest for the correlogram and PG-Capon, with BGP-Capon in between. We see that the BPG-Capon estimate is 10-20 dB lower than PG-Capon in the noise velocity range. The APES variants behave similarly but are not plotted for figure clarity. We also see the aliasing artifact at 1.5 m/s in the BPG-Capon estimate is about 20 dB lower than its counterpart in the PG-Capon estimate.

4. CONCLUSION

We proposed a high resolution spectral velocity estimator for gapped data that uses two dimensions - spatial and temporal dimensions - to solve a one dimensional spectral estimation problem. Through simulations using a realistic flow model, we show that the two dimensional estimator outperforms the pure 1-D estimators in both spectral resolution (mainlobe width) and contrast (leakage). Because uniform sampling limits the PRF of Doppler ultrasound, our proposed method has the potential to increase both the maximum detectable velocity and temporal resolution of blood flow using medical ultrasound.

5. REFERENCES

[1] P. Stoica and R. Moses, *Spectral Analysis of Signals*. Upper Saddle River, N.J: Prentice Hall, 2005.
 [2] J. Li and P. Stoica, "An adaptive filtering approach to

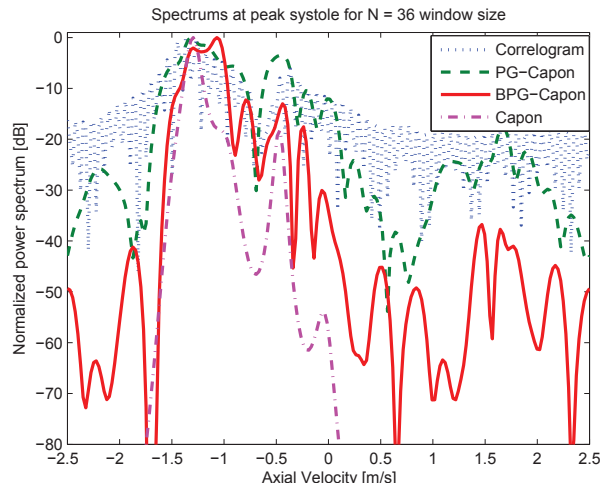


Fig. 2. Comparison of spectrums at peak systole at time 0.12s from Figure 1. Reference Capon estimator is computed with full data, while gapped data estimators are missing one out of three samples.

spectral estimation and sar imaging," *IEEE Trans. Signal Process.*, vol. 44, no. 6, pp. 1469–1484, June 1996.
 [3] F. Gran, A. Jakobsson, and J. Jensen, "Adaptive blood velocity estimation in medical ultrasound," in *IEEE International Conference on Acoustics, Speech, and Signal Processing*, vol. 1, 2007, pp. 293–296.
 [4] J. Jensen, "Spectral velocity estimation in ultrasound using sparse data sets," *J. Acoust. Soc. Am.*, vol. 120, no. 1, pp. 211–220, July 2006.
 [5] E. Larsson, G. Liu, P. Stoica, and J. Li, "High-resolution SAR imaging with angular diversity," *IEEE Trans. Aerosp. Electron. Syst.*, vol. 37, pp. 1359–1372, October 2001.
 [6] E. Larsson and J. Li, "Spectral analysis of periodically gapped data," *IEEE Trans. Aerosp. Electron. Syst.*, vol. 39, no. 3, pp. 1089–1097, July 2003.
 [7] J. Jensen and N. Svendsen, "Calculation of pressure fields from arbitrarily shaped, apodized, and excited ultrasound transducers," *IEEE Trans. Ultrason., Ferroelec., Freq. Contr.*, vol. 39, no. 2, pp. 262–267, March 1992.
 [8] J. Jensen, *Estimation of Blood Velocities Using Ultrasound: A Signal Processing Approach*. New York: Cambridge University Press, 1996.
 [9] J. Womersley, "Oscillatory motion of a viscous liquid in a thin-walled elastic tube. i: The linear approximation for long waves," *Phil. Mag.*, vol. 46, pp. 199–221, July 1955.